TSG-RAN Working Group 1 meeting #6
Espoo, Finland
July 13-16, 1999

3GPP/TSGR1#6(99)893

TITLE:

Proposal for RACH Preambles

SOURCE:

Motorola, Texas Instruments

1.0 Introduction

Several problems with the originally proposed RACH preambles based on Gold codes [1] were presented in [2]. These included 1) Large crosscorrelations between signature sequences at offsets greater than 255 chips, 2) Large crosscorrelations between signature sequences at all offsets when, due to Doppler shifts and differences between mobile TX and base RX oscillator frequencies, channel phase rotation is present, and 3) Poor estimation of the offset frequency due to this channel phase rotation caused by multiple access interference. Consequently, Nokia's proposal of using a section of a real-valued version of the uplink scrambling code as the spreading code was, in principle, accepted. This eliminates the problem of large crosscorrelations at offsets greater than 255 chips. The resulting preambles therefore consist of length 16 signature sequences formed from a set of orthogonal Gold codes spread by a 4096 chip segment section of a $2^{25}-1$ length Gold code. *The problem of large crosscorrelations in the presence of frequency offset is still however present*. This is illustrated in Fig. 1 where, for one particular long spreading code, a histogram of the maximum absolute crosscorrelations over a 2048 chip window is shown for the case of a 400 Hz frequency offset. Each point in the histogram represents one of the $\binom{16}{2}$ crosscorrelations. This contribution presents a set of preambles which eliminates this problem and, in addition, facilitates simple and accurate estimation of offset frequency as required for AFC initialization. Accurate AFC initialization based only on the received preamble is important for reliable detection of the message.

The proposed preambles have the following characteristics:

1. Low crosscorrelations at all offsets with and without the presence of channel phase rotation

2. Flexibility in detection schemes. Coherent accumulation, noncoherent accumulation, or differential detection can be used without increased crosscorrelation. *Consequently, there is no need to include a second set of preambles in the standard to facilitate differential detection.* Mobile and base station complexity as well as broadcast channel signaling is reduced.

3. Detection schemes with complexity no greater that possible needed with the present preambles.

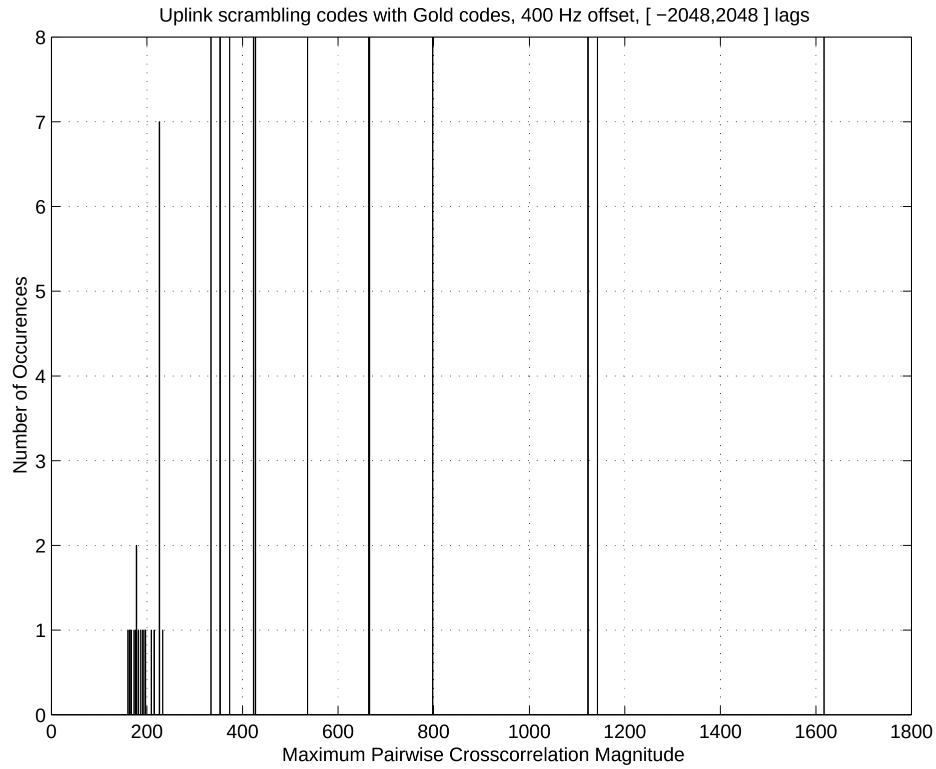

Figure 1: Maximum absolute crosscorrelations for the present preambles when a channel phase rotation of 400 Hz is present.

4. Improvement in detection performance relative to that possible with the present preambles

5. Simple offset frequency estimation without susceptibility to multiple access interference. These characteristics are discussed in detail in the following sections.

2.0 Proposed Preambles

The proposed preambles are formed from 256 repetitions of length 16 Hadamard codes multiplied by a cell-specific scrambling code consisting of a 4096 chip segment of a $2^{25}-1$ length, real-valued Gold code. Each of the sixteen preambles associated with a cell-specific scrambling code uses a different Hadamard code. The scrambling codes are formed in the same manner as the in-phase dedicated channel uplink scrambling code. The 256 different codes correspond to different initial shift register contents of one of the shift registers.

If h_m, $m = 0, 1, \cdots, 15$, is the set of length 16 Hadamard codes and c_n, $n = 0, 1, \cdots, 255$,is the set of 256 length 4096 scrambling codes, then the mth preamble, s_{mn}, corresponding to the nth scrambling code is

$$s_{mn}(k) = c_n(k) \sum_{i=0}^{255} h_m(k - 16i) . \quad (1)$$

This is illustrated in Fig. 2.

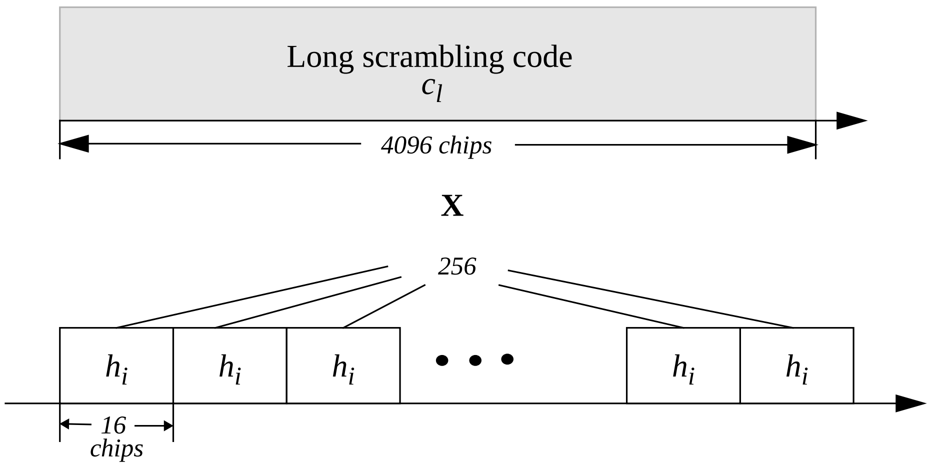

Figure 2: Structure of proposed preambles.

This structure can be viewed as a modification of the current preambles. The main difference is that in the proposed codes, the 256 chips corresponding to one symbol are interleaved at intervals of 16 across the preamble while in the current proposal all 256 chips are transmitted consecutively. In addition the 16 symbols are derived from Hadamard codes in the proposed structure instead of Orthogonal Gold codes.

3.0 Advantages of the Proposed Preambles

The proposed preambles offer three advantages over the current preambles.

3.1 Flexibility

The proposed structure allows a great deal of flexibility in the design of preamble detectors. Coherent accumulation over the entire 1ms, differential detection over some number of symbols, and noncoherent detection are all possible while specifying only one set of preambles. *The latter two methods are possible without adding an additional set of preambles* because the received preamble can be broken into segments without loss of orthogonality. For example, with the present preambles if two preambles arrive at the base within a chip and the received preamble is broken into four segments and correlations are performed over these segments, the resulting correlator outputs will contain signal energy from both users since the preambles are not orthogonal over 0.25ms segments. The noncoherent addition over the correlator outputs for the four segments will therefore contain signal energy from both users and thus a strong preamble could bias the decision statistics of weaker users. The proposed preambles however are orthogonal over 16 chip segments and therefore the correlator outputs will contain signal energy from only one user.

This flexibility has several advantages. First, because it is not necessary to have two sets of preamble codes, mobile station complexity is reduced and less signaling is required on the broadcast channel. Second, multiple detection schemes can be applied in the same sector. Noncoherent or differential detection could be used to detect high speed users while coherent detection could be used for slow speed users.

The following notation will be used in describing three possible detection schemes. Let the received preamble be denoted by $r(k)$ which is assumed to be sampled at the chip rate. This signal is multiplied by the scrambling code of the nth sector and matched filtered against the mth user's Hadamard code:

$$y_m(l) = \sum_{k=0}^{15} c_n(k+16l) r(k+16l) h_m(k), \quad l = 0, 1, \cdots, 255 \tag{2}$$

to yield a sequence of 256 matched filtered outputs.

Coherent Accumulation

Detection by coherent accumulation can be performed by summing the matched filter outputs and squaring the result to give the decision statistic:

$$\gamma_m^c = \left| \sum_{l=0}^{255} y_m(l) \right|^2 . \tag{3}$$

Noncoherent Accumulation

Alternatively, matched filter outputs can be accumulated within some number of segments of the preamble, the results squared and then accumulated. For example if the 1ms preamble is divided into four segments, the decision statistic would be:

$$\gamma_m^n = \sum_{i=0}^{3} \left| \sum_{l=0}^{63} y_m(l+64i) \right|^2 . \tag{4}$$

Differential

Differential detection may be performed by accumulating within a segment and then taking the conjugate product of consecutive sums. With four segments the decision statistic would be

$$\gamma_m^d = \left| \sum_{i=1}^{3} \left[\left(\sum_{l=0}^{63} y_m(l+64i) \right) \left(\sum_{k=0}^{63} y_m(k+64(i-1)) \right)^* \right] \right| . \tag{5}$$

Note that this statistic is somewhat different from what is usually considered with differential detection. Namely, the absolute value of the consecutive products is taken instead of the real part. As will be discussed shortly this was found to give better performance when large frequency offsets are present.

3.2 Reduction in Crosscorrelation

As illustrated in Fig. 1, the current preamble codes can have large crosscorrelations when a frequency offset is present. With coherent accumulation detection, crosscorrelation causes the decision statistics of preamble codes which are not present to take nonzero values. When the transmitted preamble is received with large signal power, these decision statistics could cross the detection threshold and cause false detections. This may occur for example when the power control error is such that the mobile overestimates the amount of power required to reach the base. A distribution of power control error which is log-normal with standard deviation of 9 dB and limited at 12 dB is suggested in [3]. To insure a low rate of false detections, a large degree of "isolation" between the decision statistics of the transmitted and non-transmitted preambles is required. This false detection phenomenon is described in more detail in Section 6 for a case where the undesired decision statistics are only 9 dB down from the desired.

The large crosscorrelations seen in Fig. 1 were found to occur at zero lag. and are investigated further in the following section.

3.2.1 Zero Lag Crosscorrelations

The decision statistics for the three detection methods discussed above are presented in Figs. 3 through 5 for frequency offsets from 0 to 1200 Hz. These plots show the 16 decision statistics when the first preamble is transmitted and the correct timing offset is being processed. In Fig. 3 the 16 decision statistics for coherent detection of the present and proposed preambles are plotted. From Fig. 3a we see that for the current preambles the decision statistic corresponding to the 14th preamble is less than 10 dB below that of the transmitted preamble at an offset of only 400 Hz. On the other hand, the decision statistics are greater than 40 dB below that of the transmitted preamble for the proposed codes for offsets up to 1200 Hz. In either case however, the decision statistic of the transmitted preamble drops off rapidly between 400 and 800 Hz. This reduction does not occur when noncoherent accumulation is used as shown in Fig. 4 where the noncoherent decision statistics of (4) are plotted. From Fig. 4a we see that noncoherent accumulation over four segments is not viable with the current preamble codes due to the low isolation between decision statistics at even 0 Hz. This is expected in that the present preamble codes are not orthogonal over.25ms. Greater than 40 dB of isolation between decision statistics is however seen with the proposed codes, Fig. 4b. Note that the decision statistic of the transmitted preamble does not drop with large frequency offsets. The case of differential detection is shown in Fig. 5. A uniform isolation of approximately 12 dB is seen for the current preambles and more than 40 dB with the proposed preambles.

3.2.2 Crosscorrelation of Proposed Signatures at Nonzero Lags

The above section described the crosscorrelation properties of the proposed codes at zero-lag. At other lags, the random property of the long code keeps the crosscorrelations small. Figure 6 shows a histogram of the maximum absolute crosscorrelations over a 2048 chip window with a 400 Hz frequency offset for the proposed preambles. Crosscorrelations are seen to be clustered at about -26 dB relative to the main peak. Comparison with the corresponding plot for the present

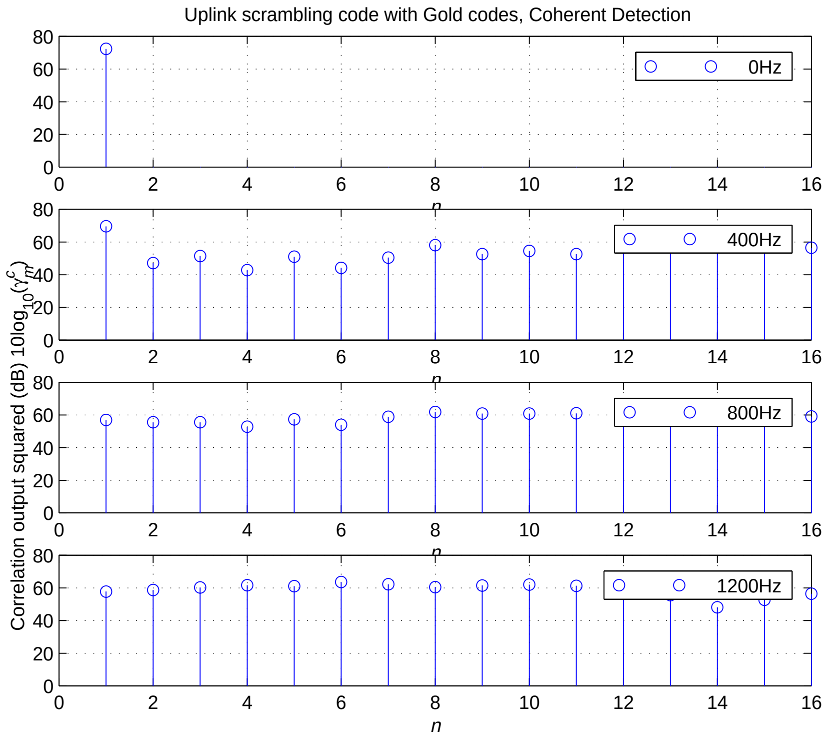

a)

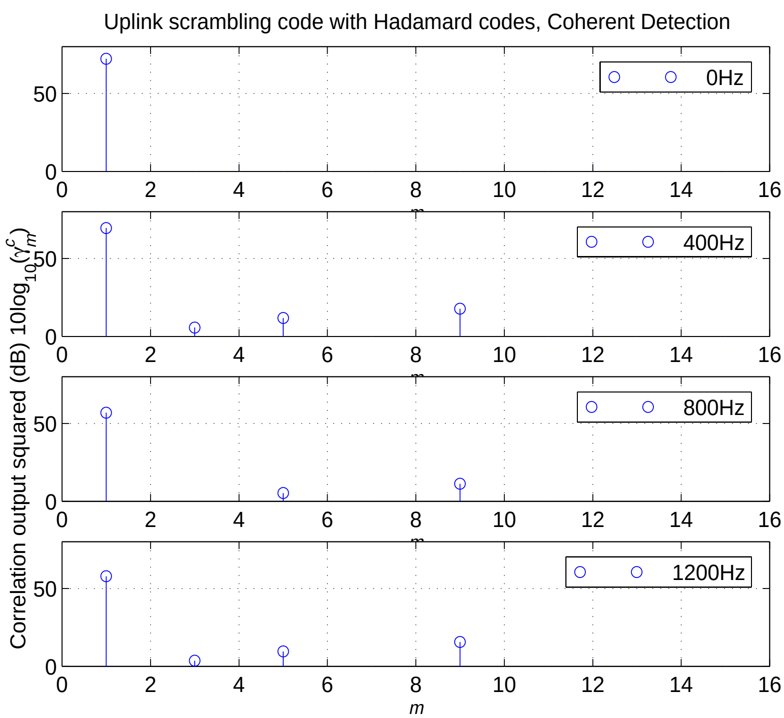

b)

Figure 3: Decision statistics for coherent detection with a) present preamble and b) proposed preambles.

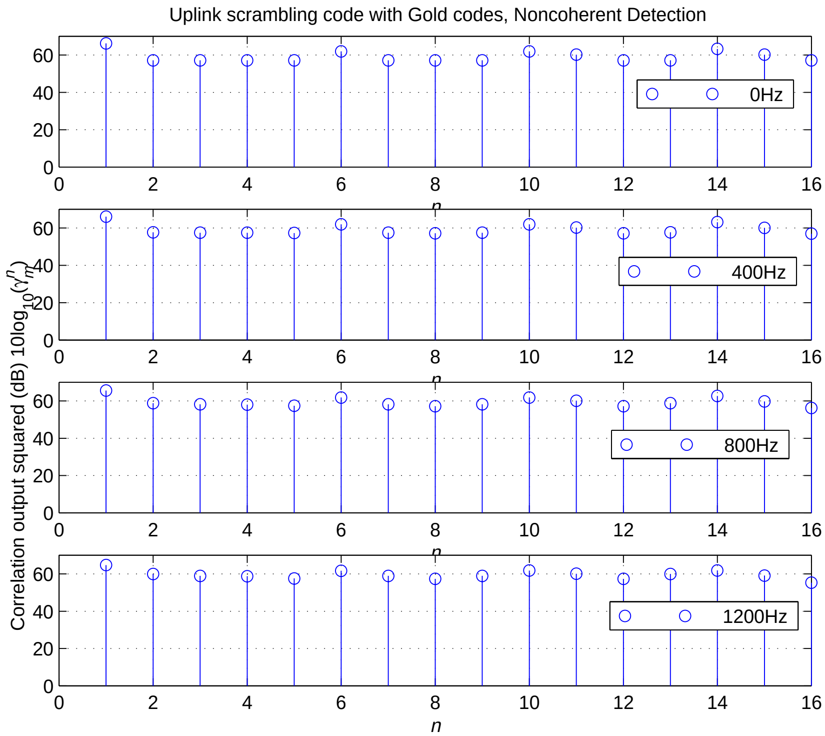

a)

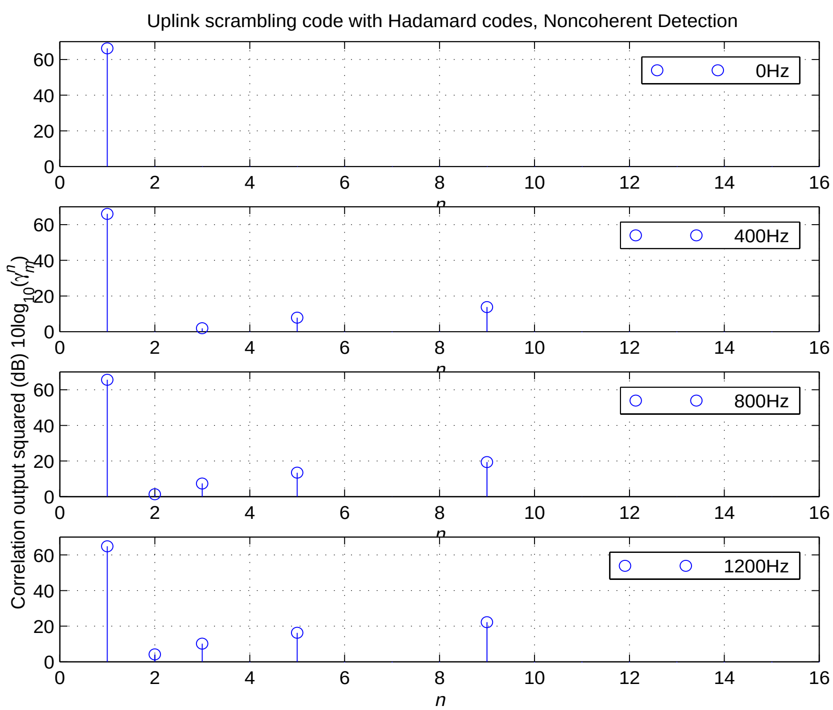

b)

Figure 4: Decision statistics for noncoherent detection with a) present non-differentially encoded preambles and b) proposed preambles.

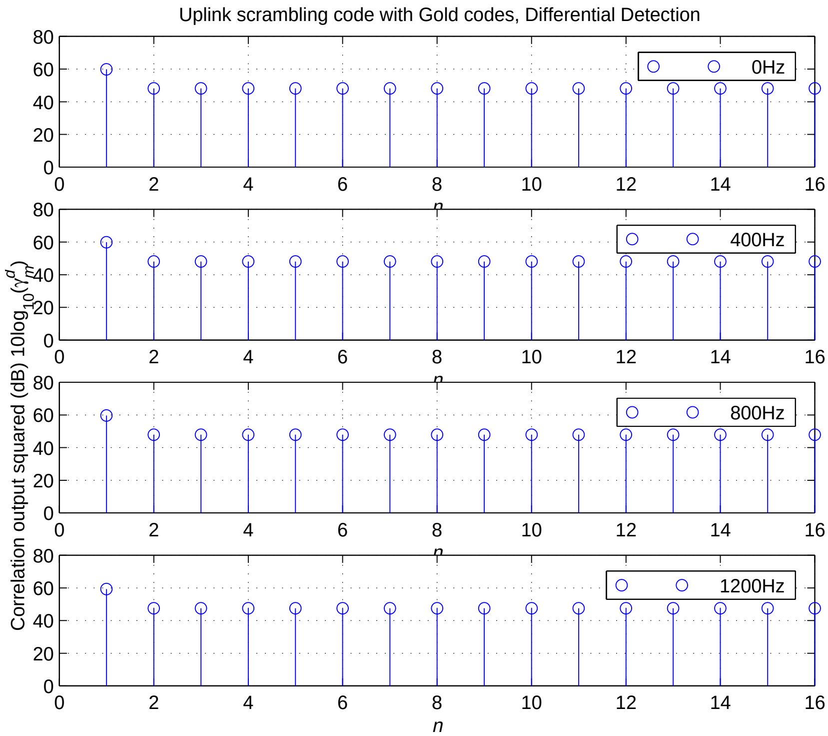

a)

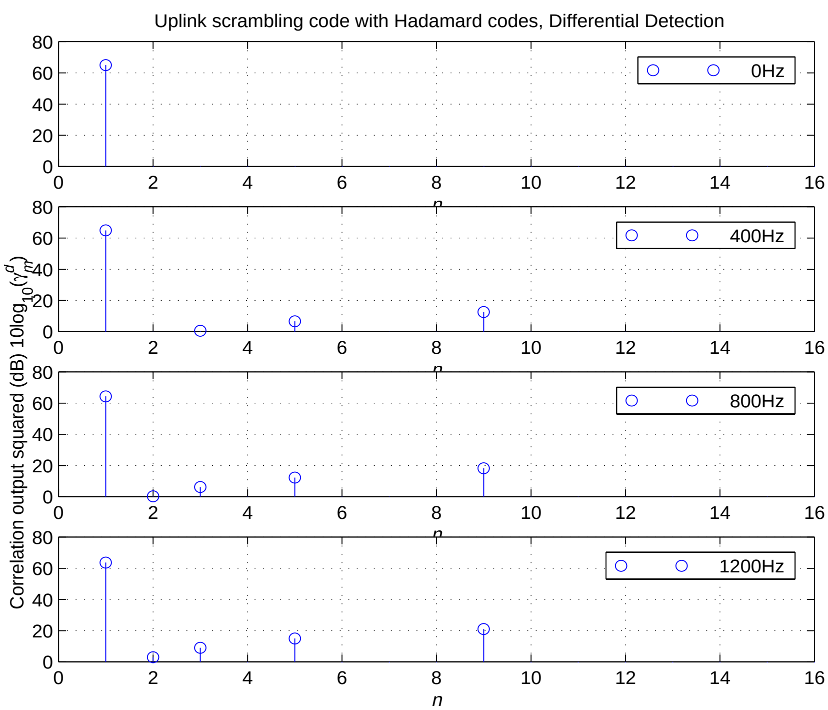

b)

Figure 5: Decision statistics for differential detection with a) present differentially encoded preambles and b) proposed preambles.

preambles, Fig. 1, shows a dramatic reduction in crosscorrelation.

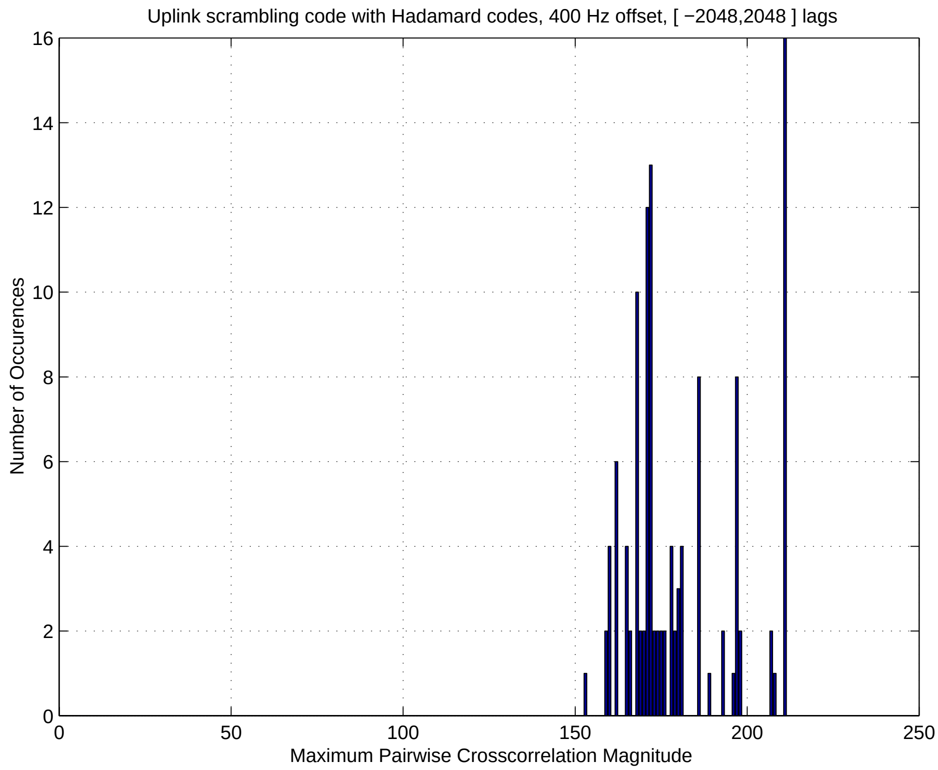

Figure 6: Maximum absolute crosscorrelations for the proposed preambles when a channel phase rotation of 400 Hz is present.

3.3 Offset Frequency Estimation

Besides increasing correlation between signature sequences, a frequency offset between the received preamble and the base station oscillator can degrade coherent demodulation of the message frame. By estimating this offset from the preamble, the receiver oscillator's frequency may be adjusted prior to message detection or the offset may be used as an initial condition for an automatic frequency control circuit. A simple method which is relatively easy to implement is based on calculating phase differences between consecutive samples [4]. Filtering or phase unwrapping can then be applied to yield the offset frequency estimate.

The structure of the present non-differentially encoded preambles however makes this relatively simple approach vulnerable to multiple-access interference from other RACH preambles. As an example consider the case of an interfering preamble with no offset which arrives with the same offset as the preamble whose offset frequency is to be estimated. Let y_k and $\bar{y}_k$ be the desired and interfering symbols respectively at time k and let θ be the change in phase between symbols corresponding to the desired offset frequency. Neglecting additive noise, the received signal is then

$$r_k = y_k e^{jk\theta} + \bar{y}_k . \tag{6}$$

The phase can be estimated by taking the argument of the filtered differences over $N = 16$ symbols:

$$\hat{\theta} = \arg z \tag{7}$$

$$\begin{aligned} z &= \sum_{k=1}^{N-1} y_k^* y_{k-1} r_{k-1}^* r_k \\ &= \sum_{k=1}^{N-1} e^{j\theta} + \bar{y}_k y_k^* e^{j(k-1)\theta} + y_{k-1} \bar{y}_{k-1}^* e^{jk\theta} + y_k^* \bar{y}_k y_{k-1} \bar{y}_{k-1}^* \end{aligned} \tag{8}$$

The term $y_k^* y_{k-1} \bar{y}_k \bar{y}_{k-1}^*$ in the above is a correlation between the new sequence, $y_k y_{k-1}$, which comes from taking consecutive products of the desired preamble and the new sequence, $\bar{y}_k y_{k-1}^*$, which comes from consecutive products of the interfering preamble. The problem comes from the fact that while cross correlations between signatures are designed to be zero, the crosscorrelations between these new sequences are generally not zero. Consequently, the last term in (8) could cause a significant bias in the estimate.

This is indeed the case for the desired and interfering signatures corresponding to signatures 0 and 2 respectively from [5]. In this case, the last interfering term has equal magnitude to the term containing the phase information. Figure 7 plots offset frequency error standard deviation vs. interfering power for this example for both the present and proposed preambles. With the present preambles degradation begins at -3 dB reaching over 1 kHz when the interfering and desired signal power are equal. With the proposed preambles however, the symbols of the interfering preambles are orthogonal to those of the desired and therefore no degradation in frequency estimation is observed with increasing interference power. Note that this does not occur if the present differentially encoded preambles are used.

.

4.0 Complexity comparison

In this section we compare the complexity of receiving the RACH preamble for the current Gold codes based preambles to the proposed Walsh Hadamard codes based preambles. We show that the complexity of the proposed sequences under all cases, that is whether are they received coherently, differentially or by segmenting is about the same as the corresponding complexity for receiving the current Gold codes based sequences. Thus, the improved performance and receiver implementation flexibility for the proposed codes is achieved without any increase in receiver complexity.

Figures 8 and 9 give the coherent receiver block diagrams for the current and proposed sequences

.

We can now do the complexity comparison for the coherent receiver for the current Gold code based scheme and the proposed Walsh Hadamard code based scheme. In our calculations we assume that the correlation outputs have to be generated over a total lag of L= 1024 chips corresponding to a cell radius of a maximum 75 Km. at an oversampling ratio of n = 2 as given in fig-

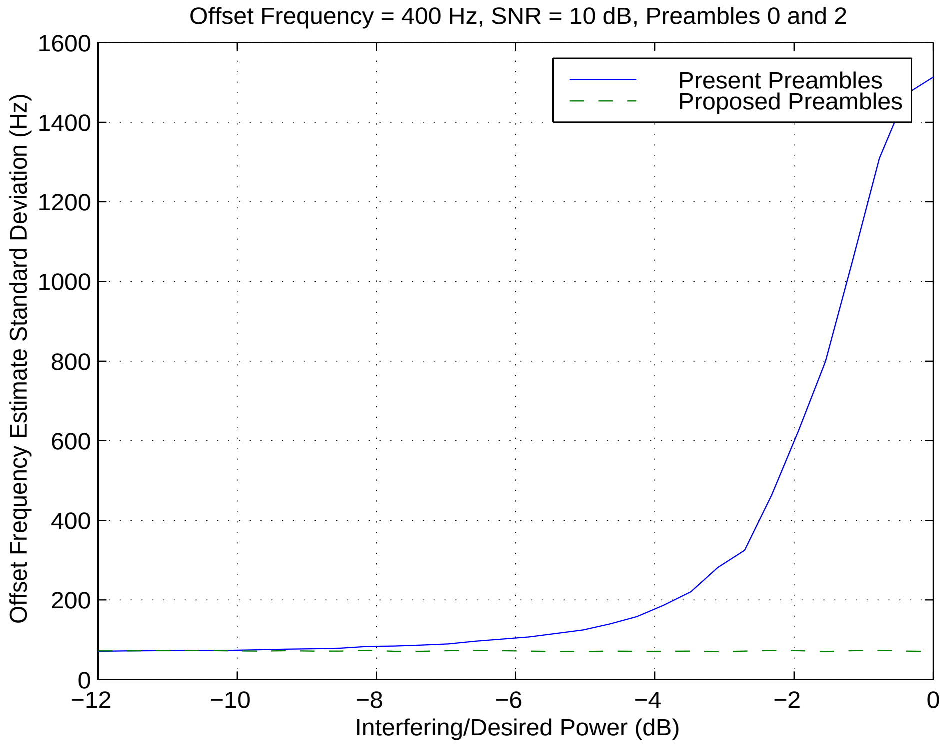

Figure 7: Effect of interfering preamble on offset frequency estimation

ure (1) and (2).

<u>Complexity calculation for the coherent demodulation for the current Gold code based approach:</u>
Number of complex adds per correlation output = 16*255+16*15 = 4320
Number of complex adds for *L* lags at n samples per chip = 4320*L*n
For L = 1024, n = 2 the total number of complex adds is = 8.9 Million complex adds

<u>Complexity calculation for the coherent demodulation for the proposed Walsh Hadamard code based approach:</u>
Number of complex adds per correlation output = 16*255+16*4 = 4144
Number of complex adds for L lags at n samples per chip = 4144*L*n
For L = 1024, n = 2 the total number of complex adds is equal = 8.5 Million complex adds

We can thus see that for the coherent demodulation the proposed Walsh Hadamard based codes have a lower complexity as compared to the current Gold code based approach.

Instead of doing the complexity calculation in detail for all the other cases, Table 1 enumerates the complexity comparison for the current Gold code based approach and the proposed Walsh Hadamard based codes for the different detection techniques:

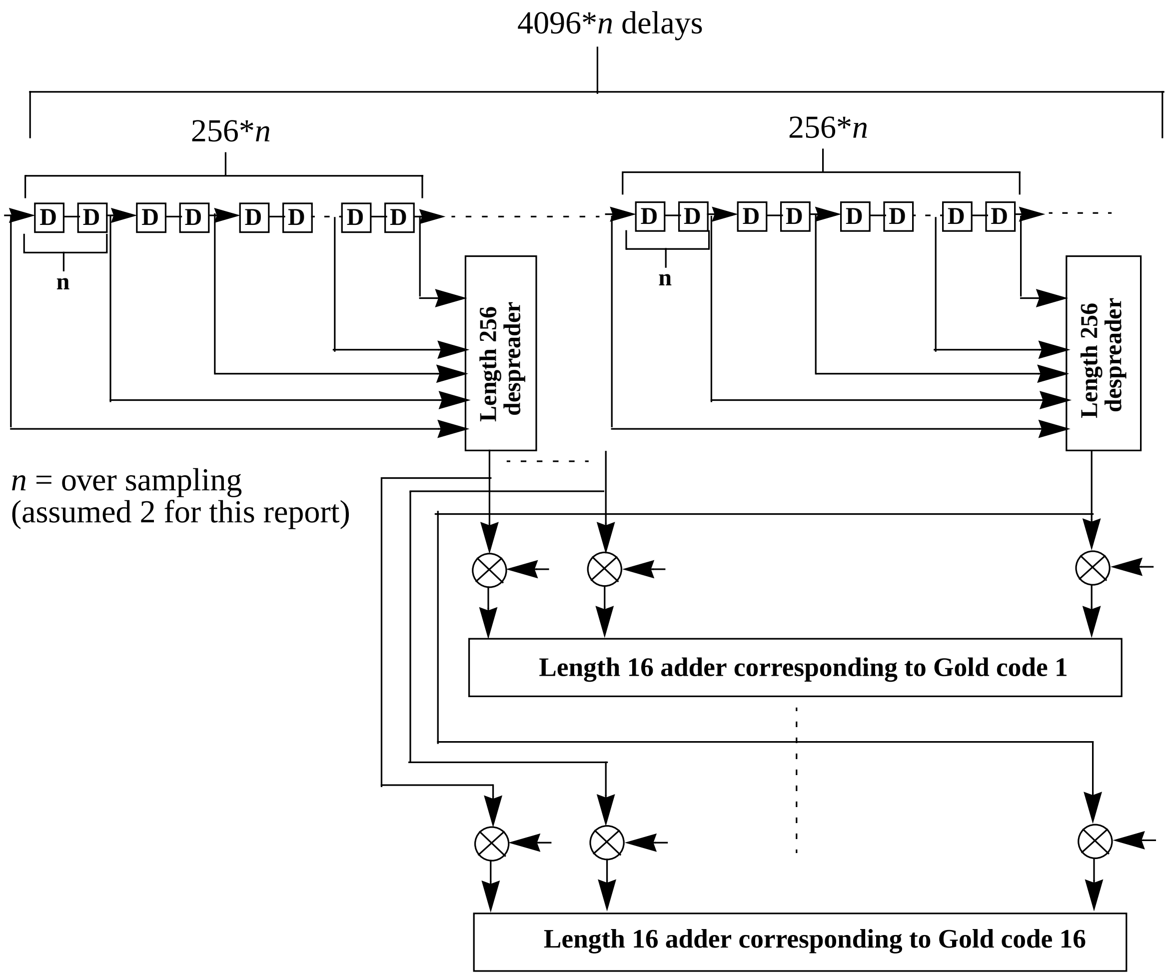

Figure 8: ***Block diagram of the preamble coherent receiver for the current Gold code based preamble. Due to the presence of a length 4096 long code on the top, a length 4096*n matched filter is required, n being the amount of over sampling and is assumed to be 2 in the complexity calculations for this report.***

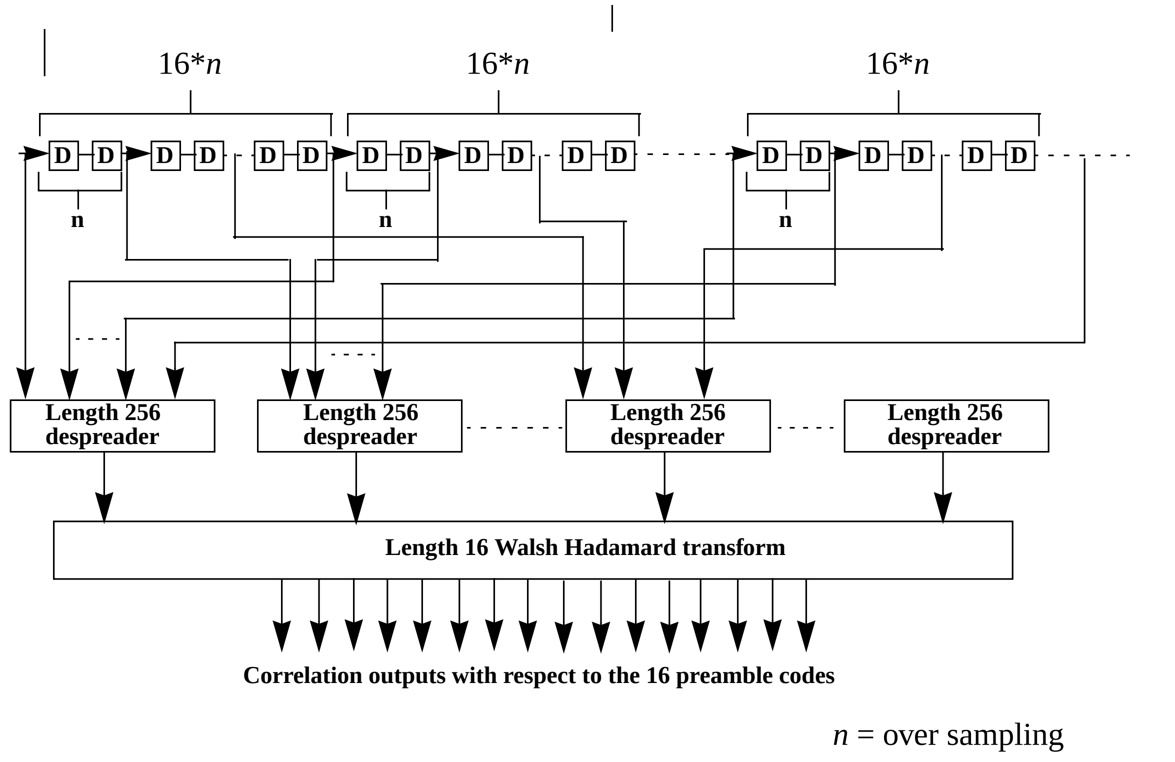

Figure 9: ***Figure 2: Block diagram of the preamble coherent receiver for the proposed Walsh Hadamard code based preamble. Due to the presence of a length 4096 long code on the top, a length 4096*n matched filter is required, n being the amount of over sampling and is assumed to be 2 in the complexity calculations for this report.***

	Current Gold code based preambles	Proposed Walsh code based preambles
Coherent reception	8.9 M complex adds	8.5 M complex adds
Differential decoding (16 for current codes and 4 for proposed)	8.9 M complex adds + 0.03 M complex multiply	9.0 M complex adds + 0.098 M complex multiply
4 segment decoding		8.9 M complex adds +.131 M complex multiply

Table 1: Complexity comparison for the different reception techniques for the current and proposed preamble codes. We can see that in all the cases, the complexity for the proposed Walsh Hadamard codes is almost the same as the corresponding complexity for the current Gold code based approach.

5.0 Detection Performance

The performance of the three detectors presented in Section 3.1 was evaluated for the present and proposed preambles in channels with frequency offset and fading. Two sets of simulations corresponding to two RACH detection scenarios were simulated. Similar results were obtained in both scenarios.

5.1 Comparison of Decision Statistic with a Fixed Threshold

In the first set of simulations the received signal at the base consisted of a single preamble plus additive noise. For each detector the decision statistic corresponding to the transmitted preamble was calculated as described in Section 3.1 and compared with a threshold to give a detection probability. The threshold was set so that when no signal was present, the probability of the statistic being greater than the threshold was equal to a false alarm probability of 0.001. In each channel four configurations are evaluated: 1) Coherent accumulation detection (identical results would be obtained in these simulations with either the present or proposed preambles) 2) Differential detection with current preambles 3) Noncoherent detection with proposed preambles and 4) Differential detection with proposed preambles.

Frequency Offset

Figures 10 through 14 show results in a nonfading channel which has a linearly increasing channel phase, i.e., a frequency offset. At 0 Hz coherent detection performs approximately 1.75 dB better than both noncoherent accumulation and differential detection with the proposed preambles and 2.5 dB better than differential detection with the current preambles. At higher offsets, coherent accumulation detection degrades significantly while the noncoherent and differential schemes' performance stays relatively fixed. At all offset frequencies, noncoherent and differential detection with the proposed preambles either outperforms or equals the performance of differential detection with the current preambles. At 400 Hz this difference is 1 dB
.

Fading

Figures 15 through 19 show results in fading channels assuming a 2 GHz carrier frequency. At speeds up to 120 km/h, coherent detection is superior by approximately 2 dB while noncoherent and differential detection with the proposed preambles is about.5 dB better than differential detection with the present preambles. At 300 km/h and 500 km/h coherent detection degrades rapidly while noncoherent detection with the proposed preambles has the best performance.

Overall, using noncoherent detection over four.25ms segments with the proposed preambles gives detection performance which is robust over both frequency offsets and rapid fading. In addition, depending on the channel type, detection with the current preambles is either equal to or inferior to that with the proposed preambles.

5.2 Maximum of Decision Statistics

Previous contributions, [6][7], have evaluated RACH detection performance in terms of the probability of the maximum decision statistic corresponding to the transmitted preamble. To cross

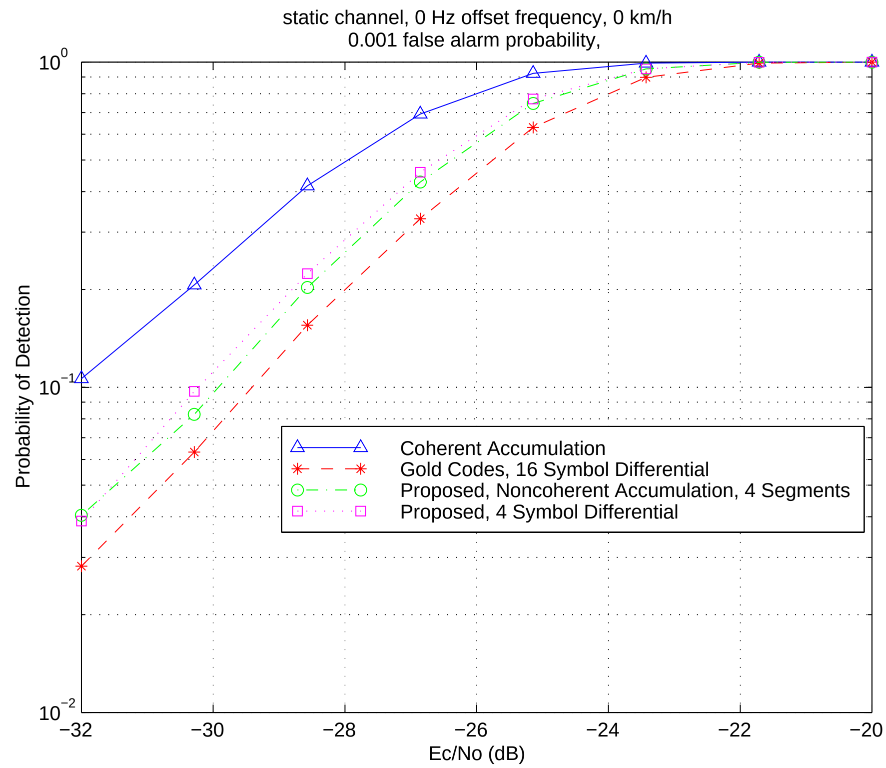

Figure 10: Static channel detection performance. No frequency offset.

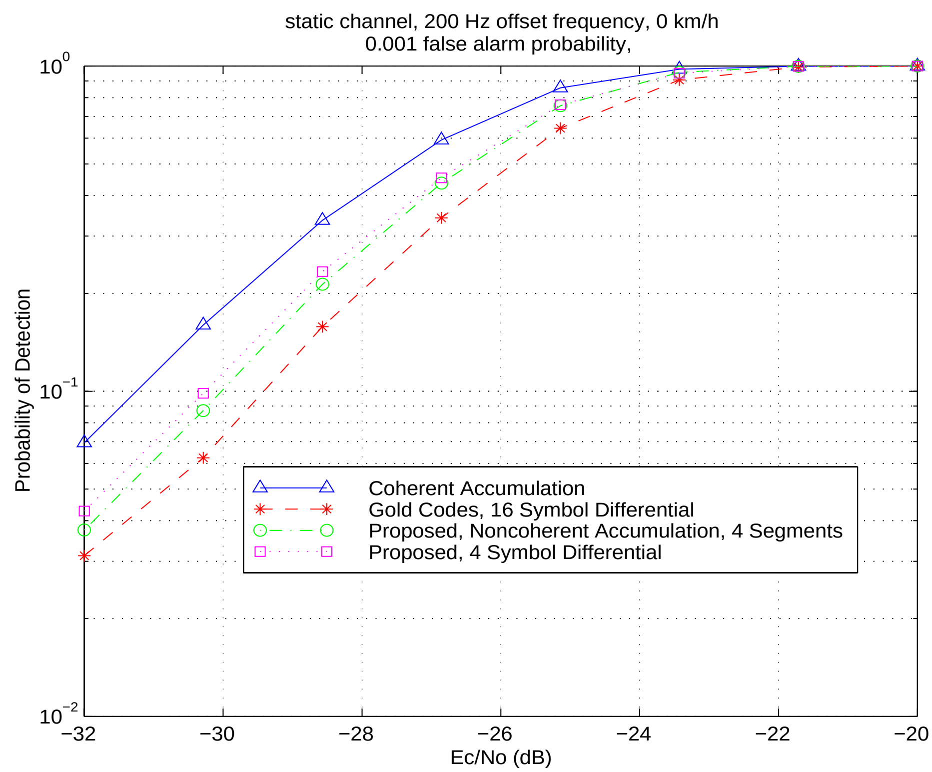

Figure 11: Static channel detection performance. 200 Hz frequency offset.

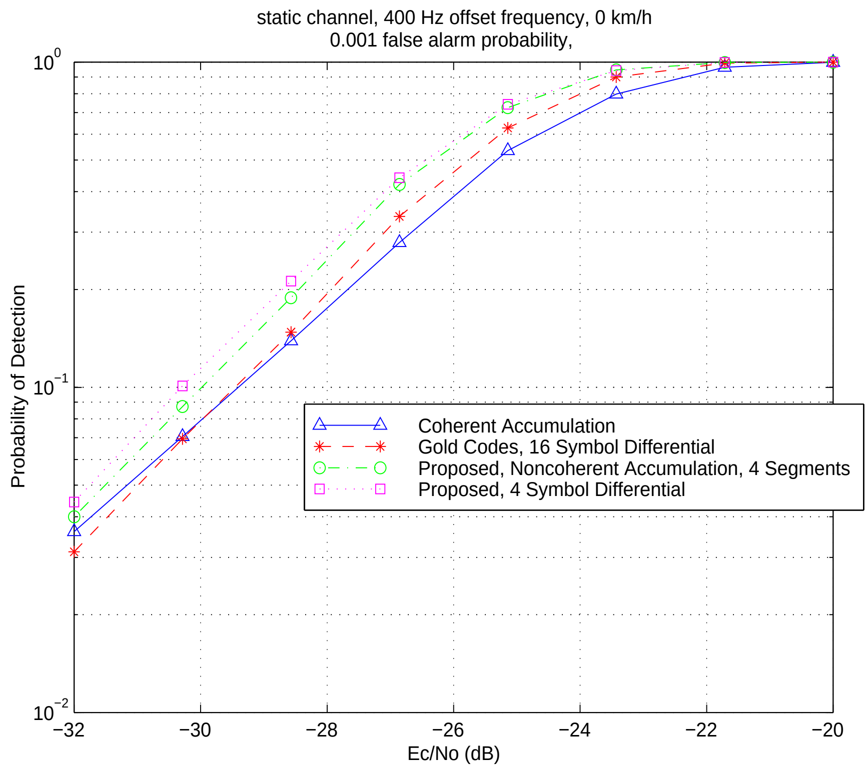

Figure 12: Static channel detection performance. 400 Hz frequency offset.

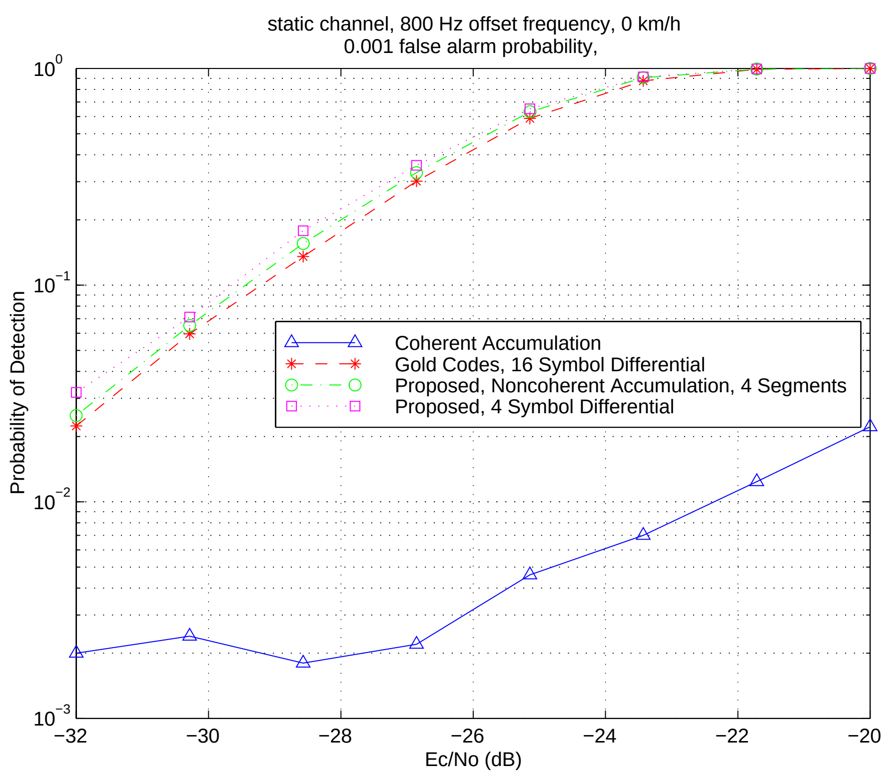

Figure 13: Static channel detection performance. 800 Hz frequency offset.

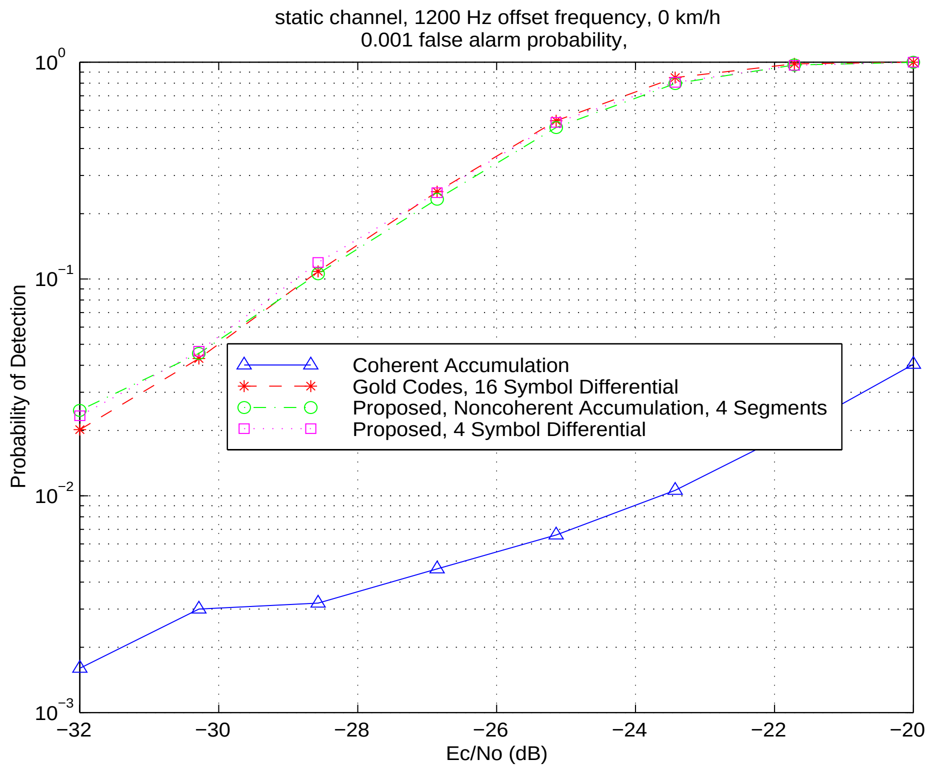

Figure 14: Static channel detection performance. 1200 Hz frequency offset.

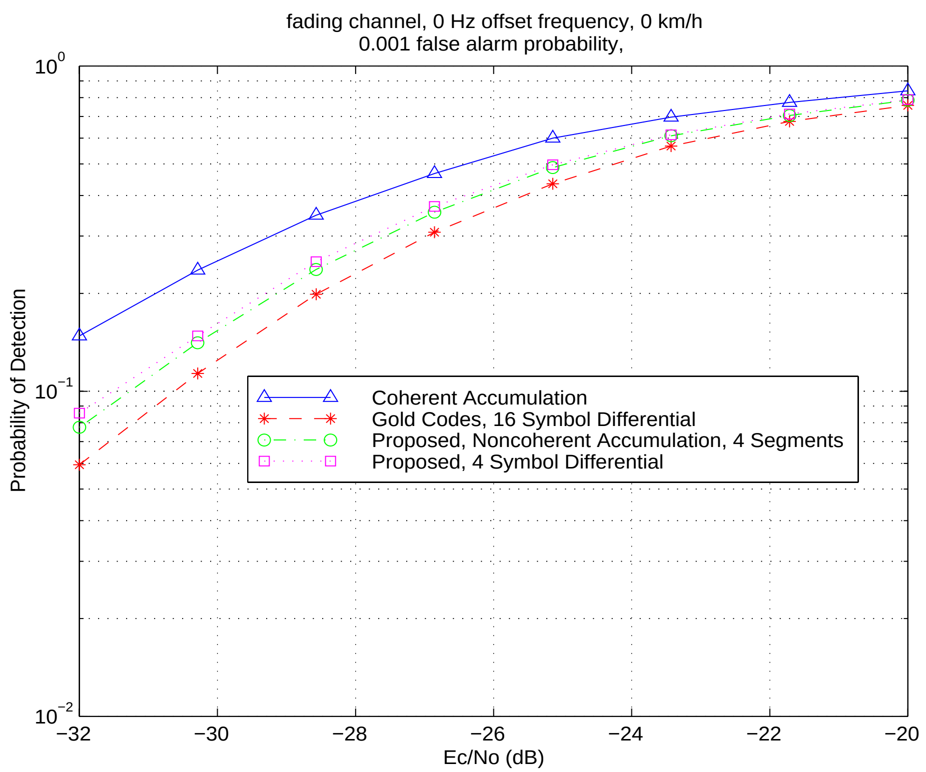

Figure 15: Fading channel detection performance. Fading is constant across preamble.

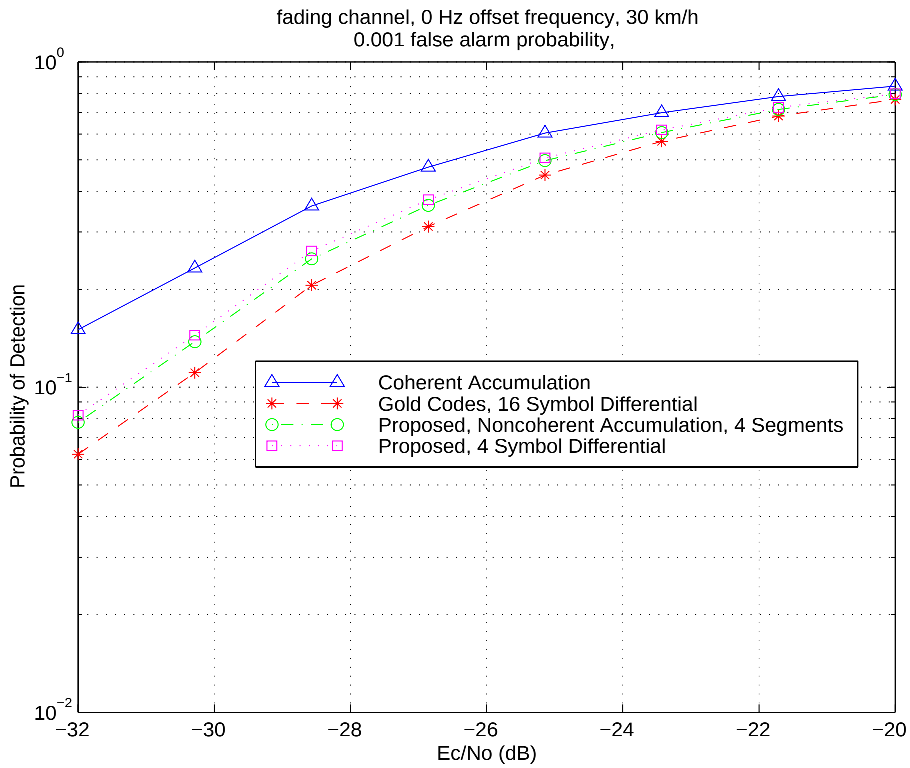

Figure 16: Fading channel detection performance. 30 km/h

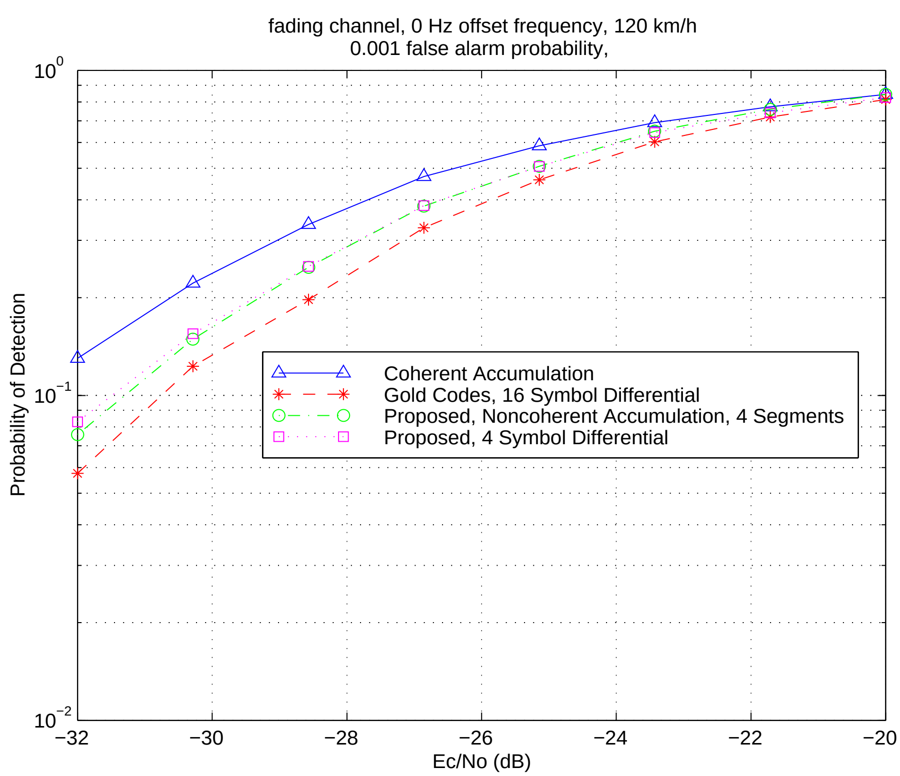

Figure 17: Fading channel detection performance. 120 km/h

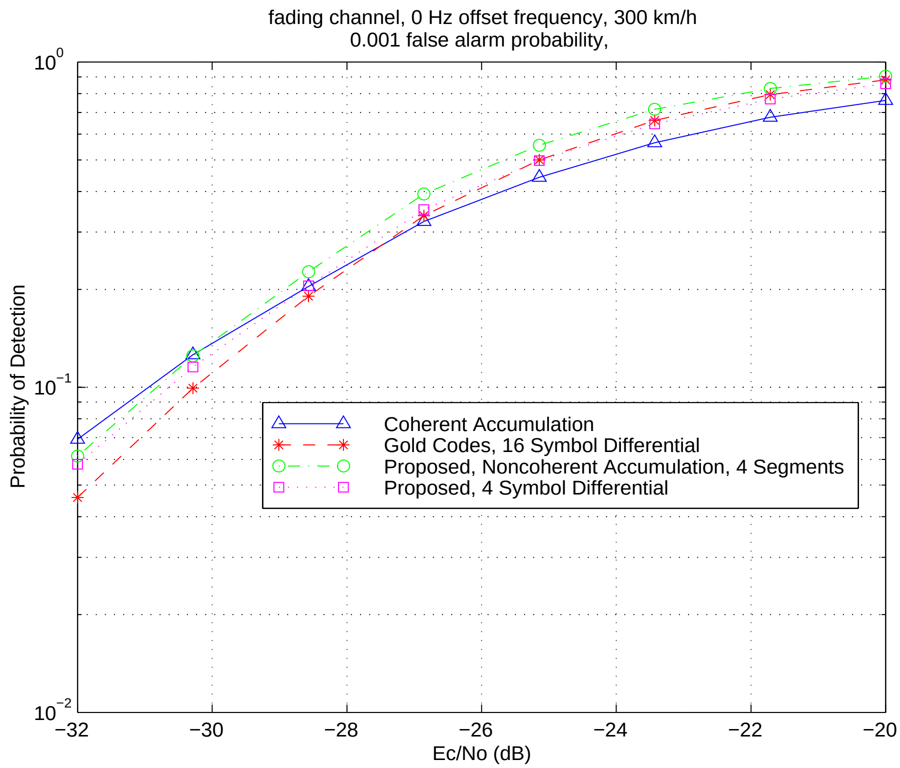

Figure 18: Fading channel detection performance. 300 km/h

check our results we ran a second set of simulation with this scenario.

Frequency Offset

Figures 20 through 24 give results in a channel with a frequency offset. Results are similar to those presented above. The coherent and differential 16 curves in Fig. 20 match those presented in Fig. 3 of [6]. Overall the relative performance of differential detection with the current preambles is seen to be worse in these scenarios than in the above. This is because of the poor isolation between decision statistics discussed in Section 3.2. Because the decision statistics of non transmitted preambles have some energy, they will tend to be detected in favor of the actual transmitted preamble. This effect is not revealed in the simulations of the previous section since only a single preamble is transmitted. Detection based on the proposed preambles is seen to be superior by about 1.5 dB over differential detection with the current preambles. The performance of coherent detection refers to coherent detection of the proposed preambles.

Fading

Figures 24 through 27 give results in fading channels. Differential detection with the current preambles is seen to be inferior to noncoherent and differential detection with the proposed preambles by 1.5 to 2.0 dB over a range of Doppler spreads. Again, the performance of coherent detection refers to coherent detection of the proposed preambles.

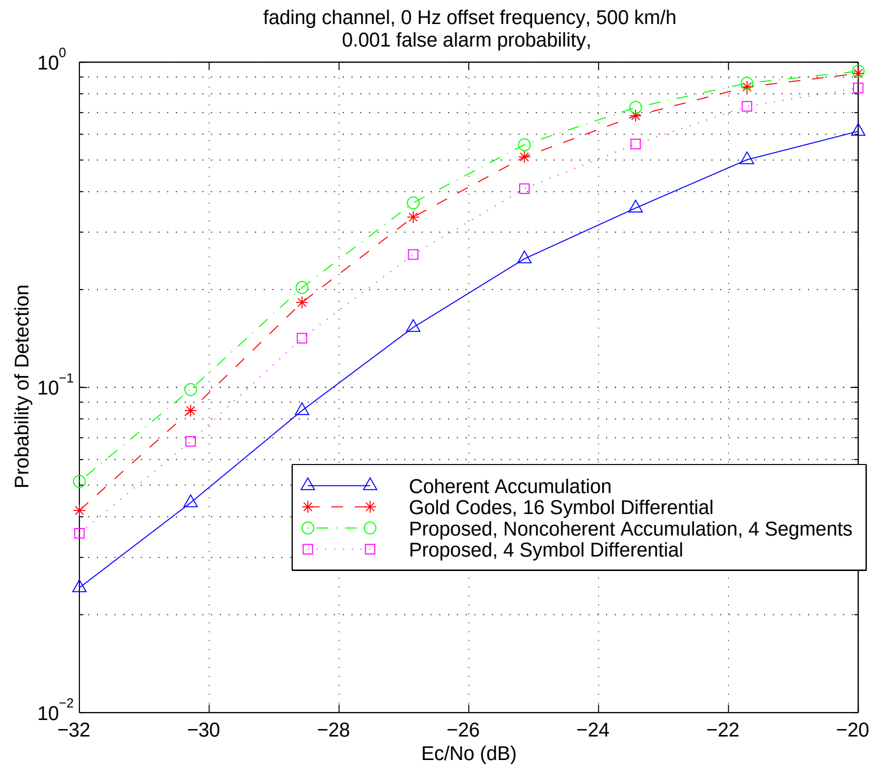

Figure 19: Fading channel detection performance. 500 km/h

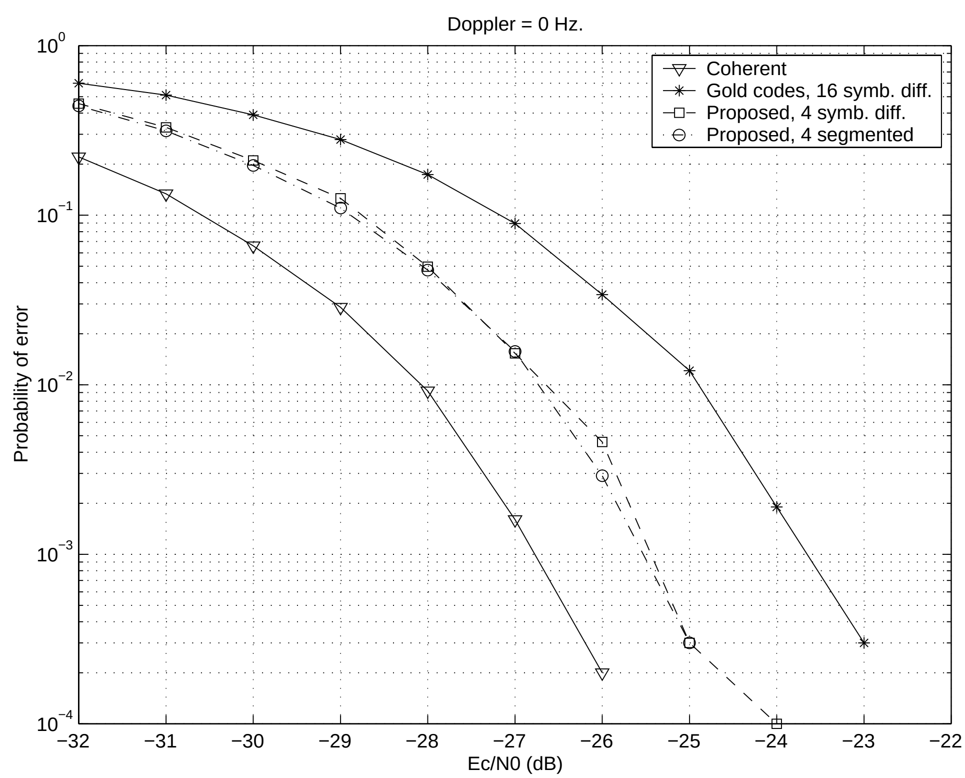

Figure 20: Probability of maximum decision statistic not corresponding to transmitted preamble. Static channel, no frequency offset.

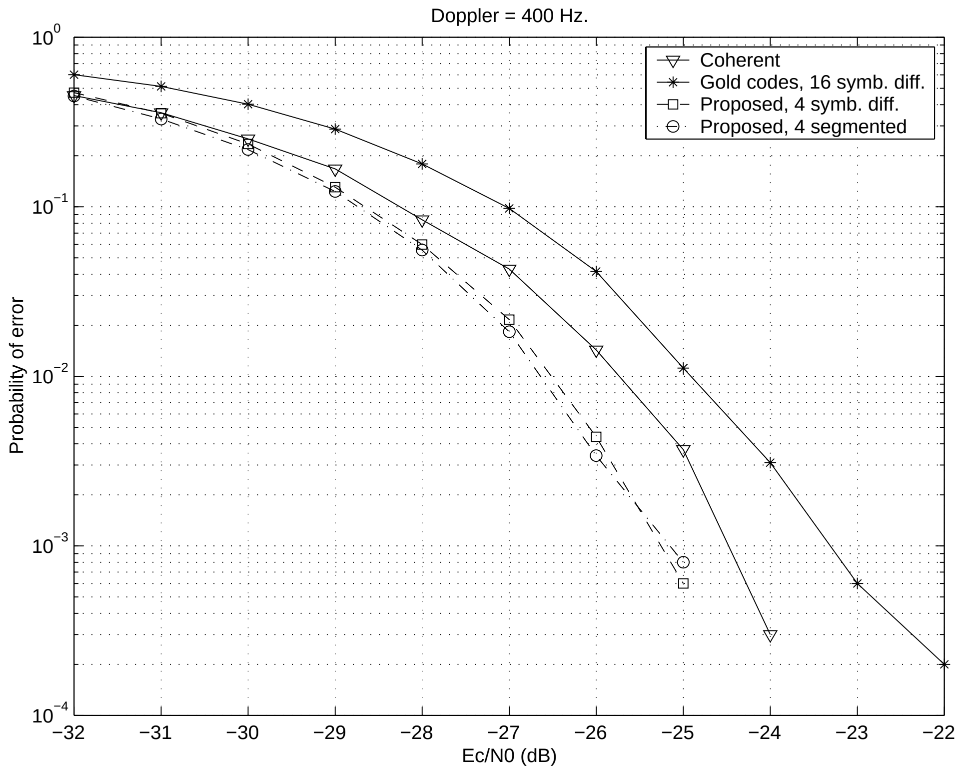

Figure 21: Probability of maximum decision statistic not corresponding to transmitted preamble. Static channel, 400 Hz offset

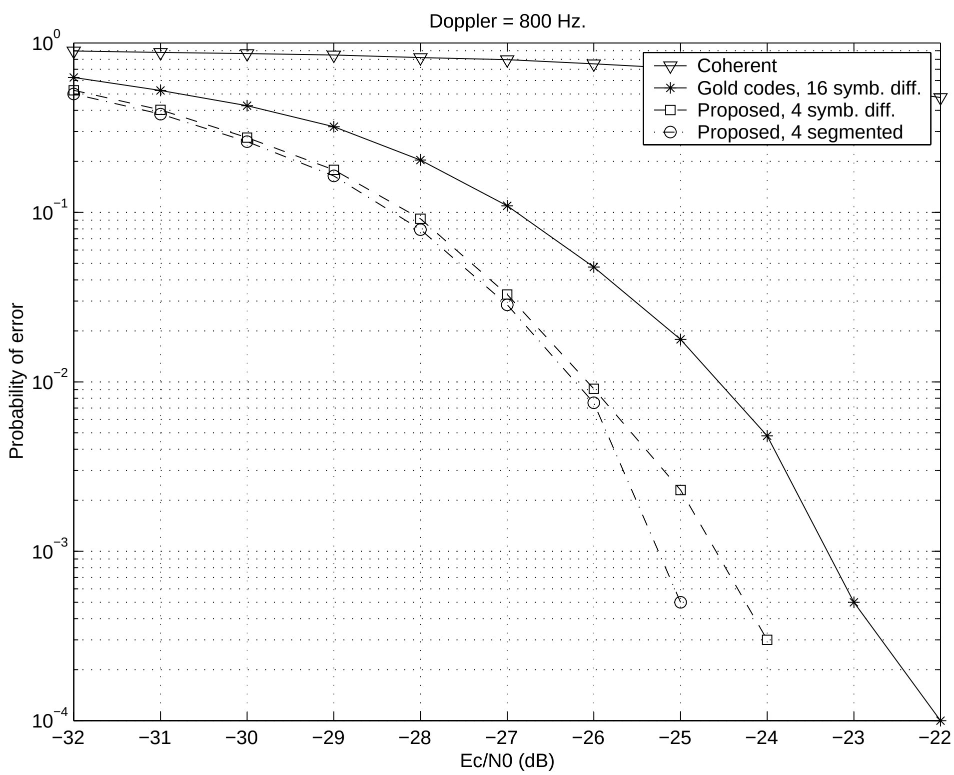

Figure 22: Probability of maximum decision statistic not corresponding to transmitted preamble. Static channel, 800 Hz offset.

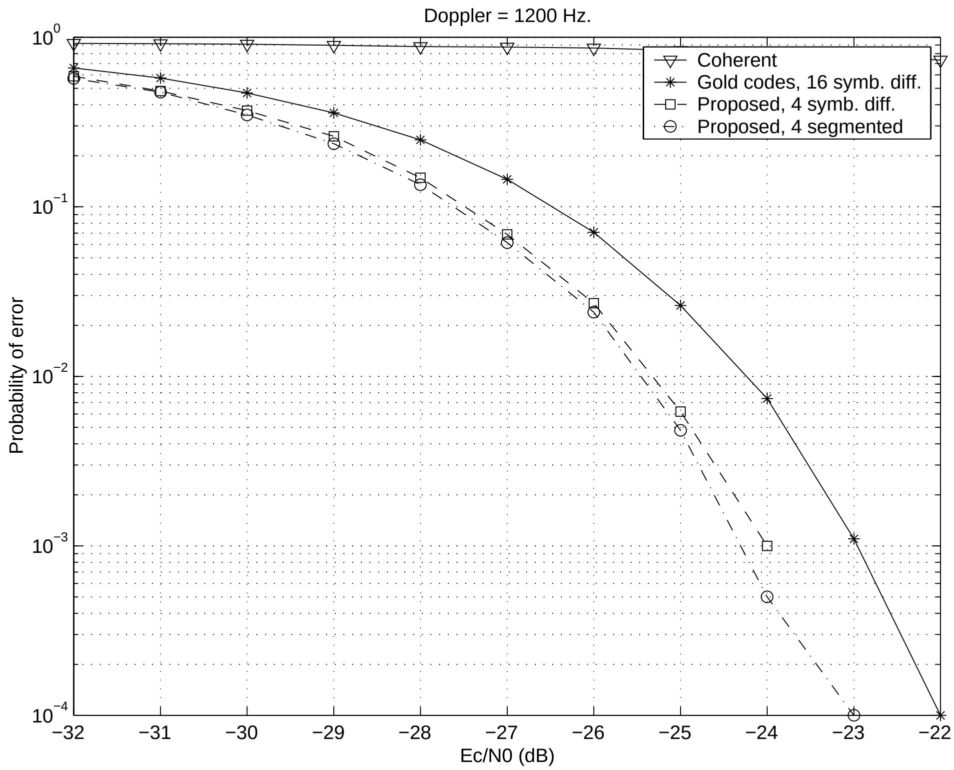

Figure 23: Probability of maximum decision statistic not corresponding to transmitted preamble. Static channel, 1200 Hz offset.

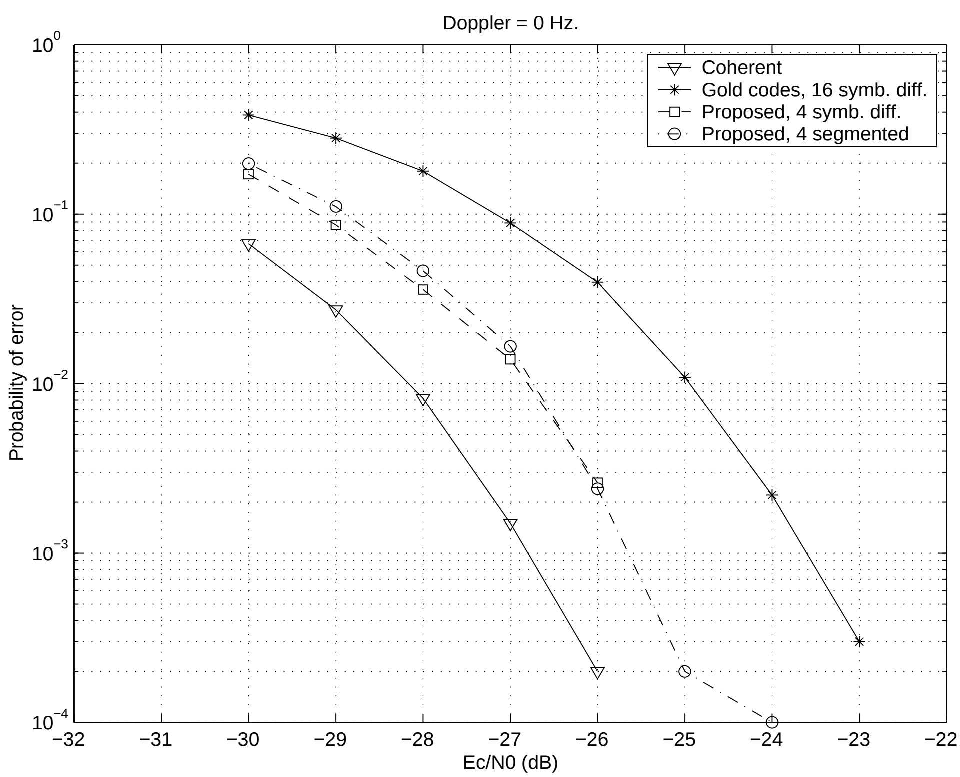

Figure 24: Probability of maximum decision statistic not corresponding to transmitted preamble. Fading channel, fading constant across preamble.

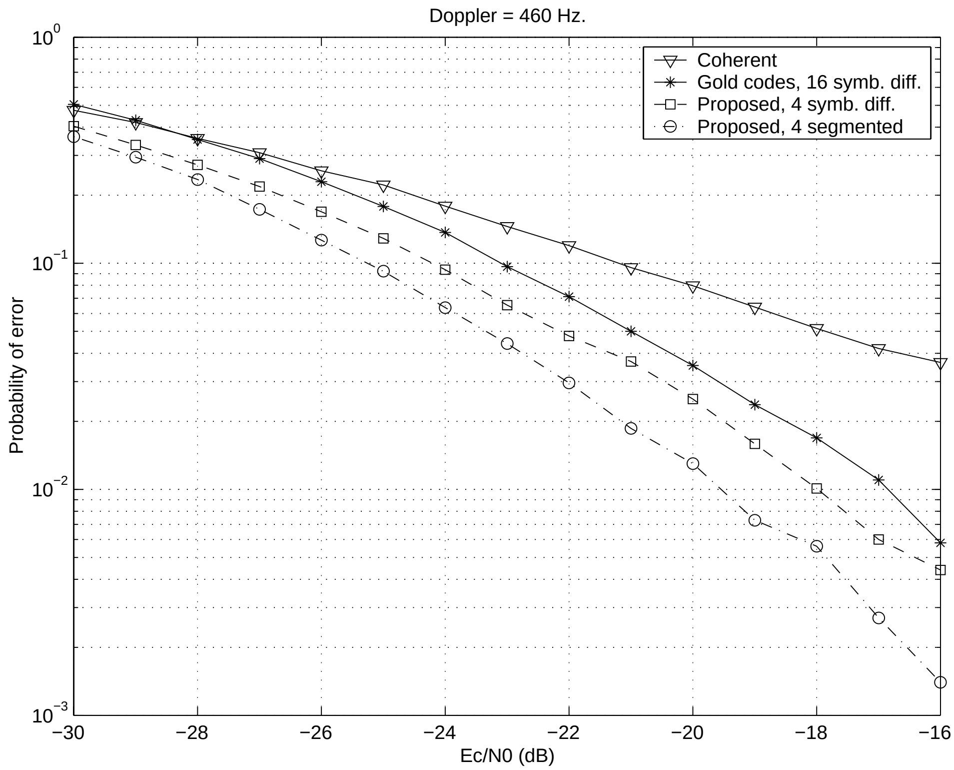

Figure 25: Probability of maximum decision statistic not corresponding to transmitted preamble. Fading channel, 250 km/h with a 2 GHz carrier frequency.

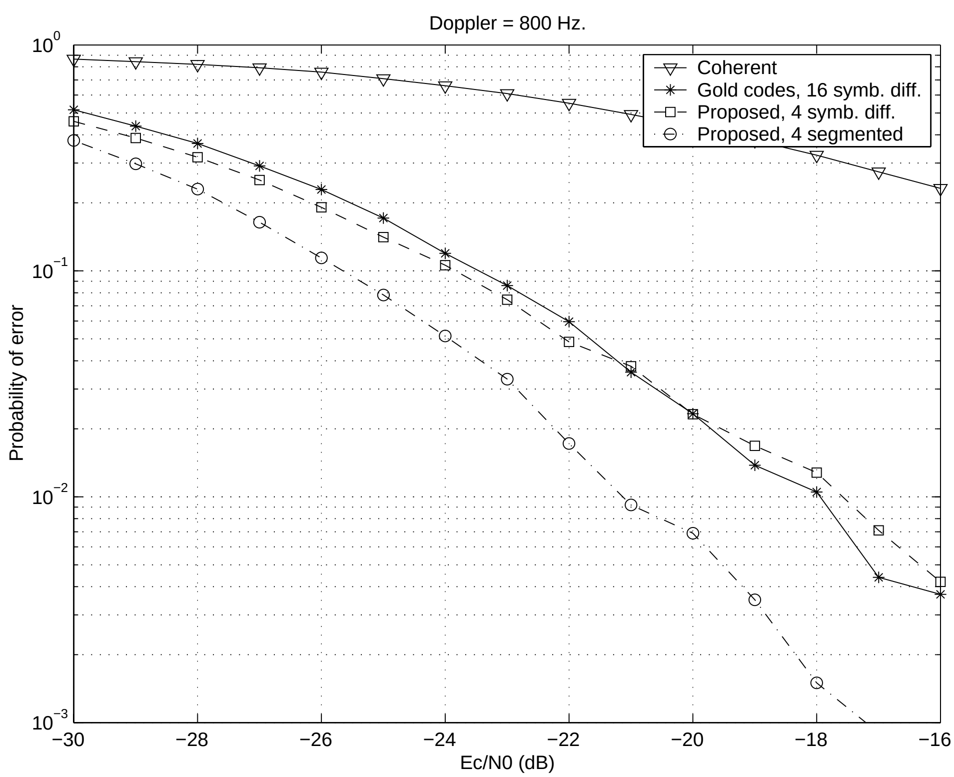

Figure 26: Probability of maximum decision statistic not corresponding to transmitted preamble. Fading channel, 430 km/h with a 2 GHz carrier frequency

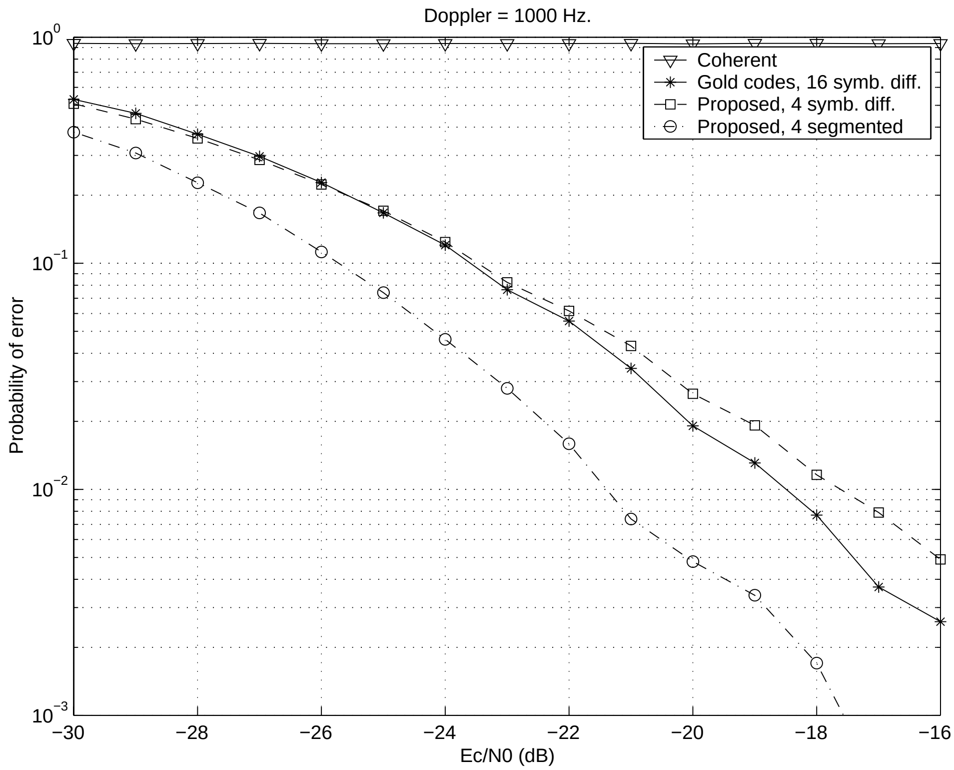

Figure 27: Probability of maximum decision statistic not corresponding to transmitted preamble. Fading channel, 540 km/h with a 2 GHz carrier frequency

6.0 Note on Inflexibility of Current Preambles

As discussed above the proposed preambles allow for either coherent and differential detection. A similar claim was made in [7] where it was noted that specifying the signatures associated with differential detection does not preclude performing coherent detection. While this is true, the resulting rate of false detections would be quite poor. The differential signatures are obtained by differentially encoding a set of orthogonal sequences so that when differential decoding is performed, the resulting length 15 sequences are nearly orthogonal. Without differential decoding however, this set of signatures has large crosscorrelations. This is shown in Fig. 28 where the decision statistics for coherent detection of the differentially encoded preambles are plotted. Isolation is seen to be less than 10 dB through 400 Hz. These large crosscorrelations will tend to cause false detections when power control errors are present. This can be seen in Fig. 29 where the probability of at least one false detection is plotted versus *Ec/No* for coherent detection of both the present differential preambles and the proposed preambles. With the proposed preambles, false detections occur at the false alarm rate while with the differential preambles, a significant number of additional false detections occur. If the target *Ec/No* point is -28 dB corresponding to a detection probability of 50% (see Fig. 10), then at the one standard deviation point of power control error, +9 dB, false detections will occur 50% of the time. It is really only feasible therefore to use differential detection when the differentially encoded preambles are transmitted

.

7.0 Conclusion

This contribution introduced a new set of preambles which are, effectively, interleaved versions of

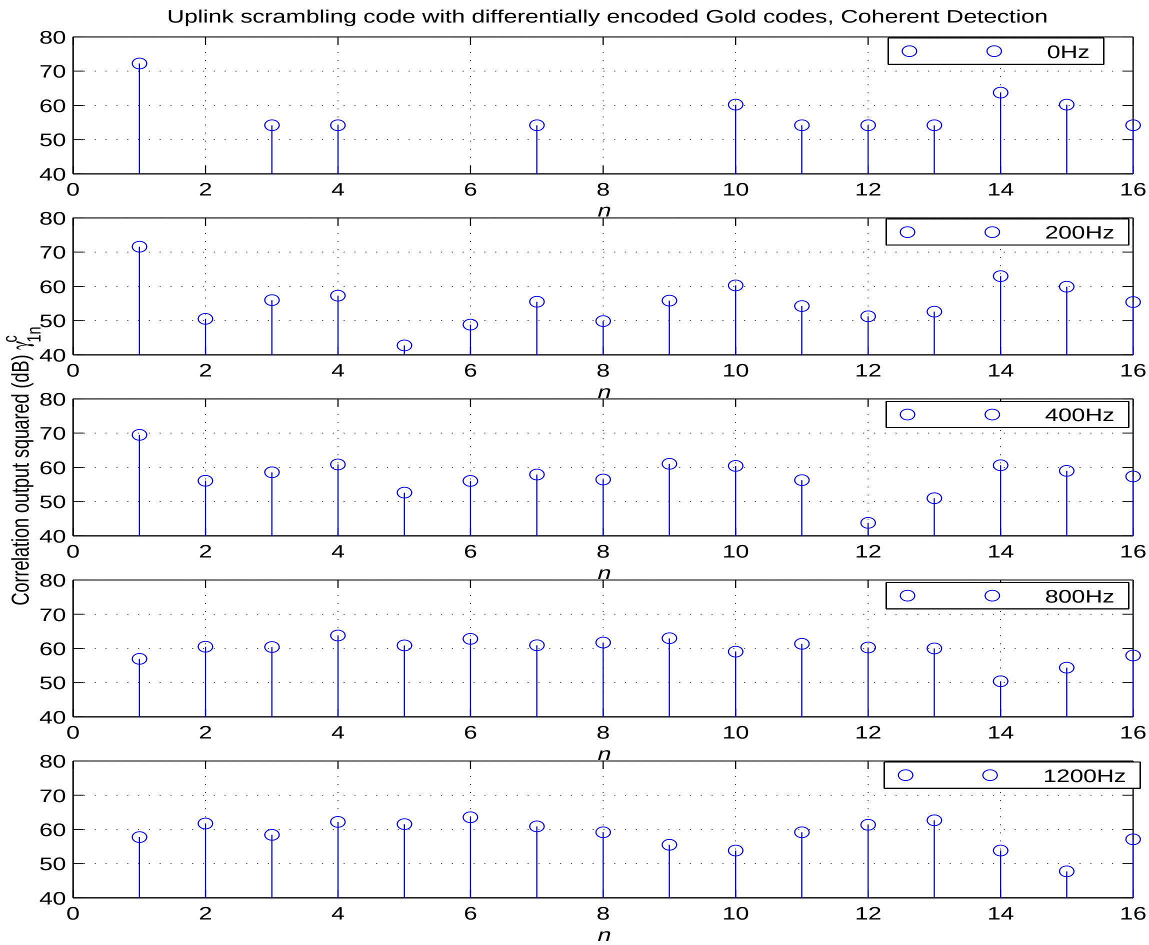

Figure 28: Decision statistics when coherent detection is performed with present differentially encoded preambles.

the present preambles. This interleaving accomplished three things: 1) Crosscorrelations between preambles in channels with frequency offset are reduced from unacceptably high values (for coherent and noncoherent detection) to nearly zero. 2) Allows the offset frequency to be accurately estimated without using differential decoding from the preamble with a simple phase delta calculation 3) Allows flexibility in the choice of detection strategies without need for multiple sets of preambles. One choice of these strategies has been shown to be equal to or superior under all channel conditions to differential detection based on the current differentially encoded signatures. In addition the proposed preambles cause no increase in detector complexity. Finally, the proposed set of 16 preambles can easily be extended to larger sets by simply using higher order Hadamard codes.

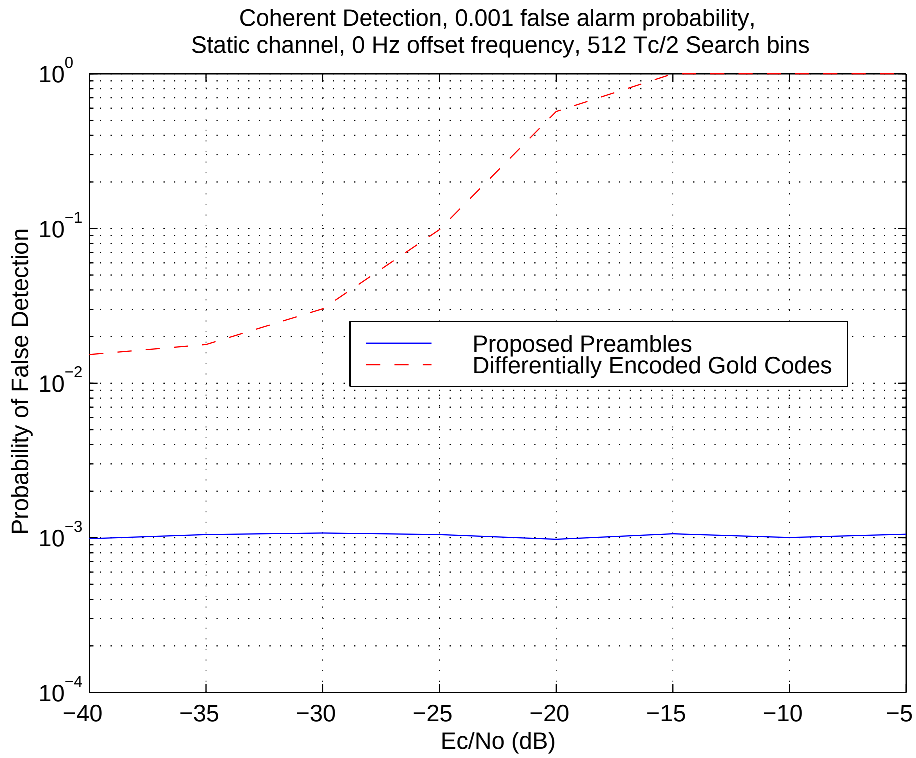

Figure 29: Probability of false detection when coherent detection is performed on present differentially encoded preambles.

8.0 References

[1] Document S1.13, v 0.1.0

[2] Evaluation of Proposed RACH Signatures, TSGR1#5(99)670, Motorola

[3] Further Discussions on Power Ramping for Random Access, Tdoc SMG2 UMTS L1 17/99, Ericsson.

[4] H. Meyr et al, Digital Communication Receivers, ch. 8, New York: Wiley Interscience., 1998.

[5] Document 25.213 v 2.1.0, TSG-RAN#4 RP99324

[6] Comparison of Detection Methods for RACH Preamble Signatures, TSGR1#3(99)140, Inter-digital Comm. Corp.

[7] Random Access Preamble Detection in Presence of Doppler, Tdoc SMG2 UMTS L1 620/98, Interdigital Comm. Corp.